

## Grazing Incidence Diffraction of keV Helium Atoms on a Ag(110) Surface

N. Bundaleski, H. Khemliche, P. Soullisse, and P. Roncin

CNRS, Laboratoire des Collisions Atomiques et Moleculaires, UMR 8625, Universite Paris-Sud, Orsay, F-91405, France

(Received 8 August 2008; published 24 October 2008)

Diffraction of fast atoms at grazing incidence has been recently demonstrated on the surface of alkali halides and wide band gap semiconductors, opening applications for the online monitoring of surface processes such as growth of ultrathin layers. This Letter reports energy resolved diffraction of helium on Ag(110) metal surface showing that a band gap is not mandatory to restrict the decoherence due to electron-hole pair excitations by the keV projectile. Measurement of the energy loss, which is in the eV range, sheds light on the scattering process.

DOI: [10.1103/PhysRevLett.101.177601](https://doi.org/10.1103/PhysRevLett.101.177601)

PACS numbers: 79.20.Rf, 34.20.Cf, 73.20.At

Heavy particle diffraction is certainly one of the most spectacular manifestations of quantum mechanics. It also offers a direct link between the microscopic world where the short wavelength probes fine details and the macroscopic world where far field diffraction diagram is recorded. Since the first observation of electron diffraction on crystals [1], shortly followed by that of He and H<sub>2</sub> at thermal energies [2], particle diffraction has become the basis of powerful surface science techniques. Usually diffraction is best observed in the quasielastic regime so that energy filtering is sometimes mandatory to improve the signal quality as for instance, in low energy electron diffraction where the inelastic contribution may be substantial. In typical experimental conditions for thermal energy atom scattering (TEAS), the 10–100 meV energy prevents electronic excitations and even phonon exchange is limited, thus leaving the elastic channel dominant. The main source of decoherence is due to random phase shift induced by thermal displacement of the surface atoms [3]. This induces an attenuation of the coherent intensity known as the Debye-Waller factor [4]  $I = I_0 \exp(-\langle(\Delta\mathbf{k} \cdot \mathbf{u})^2\rangle)$ , involving the projectile wave vector change  $\Delta\mathbf{k}$  and the mean thermal displacement  $\mathbf{u}$ , the brackets denoting thermal averaging. The diffraction intensity drops rapidly with incident energy so that even at low surface temperatures, 100 meV was considered as an upper energy limit for helium diffraction. This was true until the recent discovery of diffraction from alkali-halides at energies up to few keV at grazing incidence [5–7]. This surprising situation has been explained as due to the multiple collision regime specific to grazing scattering. In this geometry the momentum exchange with the surface atoms is distributed over many surface lattice sites allowing a separation of the motion parallel and perpendicular to the surface (see below). This transforms the surface into a set of furrows parallel to the beam on which the wave, associated with the slow motion normal to the surface, diffracts. At finite temperature, the averaging of the fluctuation of the individual position along the furrows considerably increases

the Debye-Waller factor [8,9] allowing diffraction at eV normal energies.

Yet, in contrast to thermal atom diffraction, the fast motion parallel to the surface strongly enhances the probability of the surface electronic excitations [10,11], introducing an additional source of decoherence. Excitations of surface plasmons can be excluded because the projectile does not carry any potential energy and its velocity is by far too low for a direct excitation of these collective modes [12]. Grazing incidence fast atom diffraction (GIFAD) has first been observed on large band gap ionic crystals where it is well established that no electronic excitation occur below a collision energy threshold [13,14]. Recently, similar results have been obtained on ZnSe(100) [15] suggesting that a band gap of 2.6 eV is large enough to reduce the probability for electronic excitations. The situation appears much less favorable for metals since there is no threshold energy for excitation of electrons close to the Fermi level. As the normal energy is increased, reflection from the surface takes place at shorter distances to the surface where electron densities increase as does the likelihood of these electronic excitations. The question is how likely are these excitations and how do they contribute to decoherence? More pragmatic, is GIFAD applicable to metals?

Only few experiments have reported energy loss of keV atoms on metals. Recently, Lederer *et al.* [16] have scattered 1 keV He<sup>0</sup> on clean Al(111) and measured energy losses close to 10–15 eV. Assuming that a single electron is excited, this corresponds to 1 a.u. of momentum ( $\sim 2 \text{ \AA}^{-1}$ ), exceeding the value of a typical reciprocal lattice vector, suggesting that the diffraction signal should be completely blurred out. We show in this Letter that He atoms between 300 eV and 2 keV produce well resolved diffraction patterns on Ag(110). These unexpected results demonstrate that the presence of a band gap is not mandatory to ensure coherent scattering. Energy resolved diffraction measurements suggest a possible explanation and should trigger improved theoretical descriptions of the surface electronic structure.

The Ag(110) surface was prepared by cycles of large angle sputtering with  $\text{Ar}^+$  at 500 eV while rotating the sample along the azimuth and annealing to about 600 K, followed by grazing incidence sputtering by 5 keV  $\text{Ar}^+$ . The surface was probed by a  $^3\text{He}$  beam, at energies between 300 eV and 2 keV. The primary ion beam extracted from an ECR ion source is resonantly neutralized in a He gas cell and then collimated before impinging the surface between 0.5 and 2 deg. incidence angle. The scattered helium particles hit a position sensitive detector located downstream so that the whole scattering diagram is recorded without any scan. To better understand the contribution from inelastic processes, the primary ion beam can be chopped before neutralization, allowing simultaneous measurement of the energy loss. Before addressing this energy loss issue a rapid analysis of the diffraction signal is presented to recall the specificity of this new technique.

The Z direction is normal to the surface while X and Y are in plane with Y normal to the beam,  $\mathbf{k}$  is the initial projectile momentum and  $\mathbf{G}$  a surface reciprocal lattice vector. At keV energies  $|k|$  is larger than  $|G|$  by orders of magnitude. For a frozen ideal surface, the projectile fast motion parallel to the surface (X direction) can be decoupled from the much slower one in the Y and Z directions. The argument is twofold. First, the energy associated to the exchange of a reciprocal lattice vector  $\mathbf{G}$  contains the scalar product  $|\mathbf{k} \cdot \mathbf{G}|$  that, because  $k \gg G$ , represents a much higher energetic cost for the exchange of a  $\mathbf{G}$  component parallel to the beam than perpendicular to it [6]. Second, along a low-index crystallographic axis the successive lateral deflections (Y direction) may add up to produce a large net momentum transfer. At variance along the beam direction (X) the successive slowing down and reacceleration, as the projectile flies over surface atoms, cancel each other [17]. As a result, the projectile-surface system formally acquires translational symmetry along the X direction, transforming the egg-box shape of the surface potential into its average along this direction, i.e., a corrugated iron plate surface on which the wave associated with the slow motion (YZ plane) diffracts. Note that the beam probes the averaged corrugation perpendicular to its own direction. To avoid confusion with TEAS notations, we label the results according to the probed direction rather than to that of the beam. As in any diffraction technique the information from the scattering profile is dual, the peak spacing provides structural parameters while the intensity distribution relates to the form factor, here the shape of the iron plate. Scattering profiles measured with the He beam perpendicular to (i.e., probing) the directions  $[1\bar{1}1]$ ,  $[1\bar{1}0]$  and  $[001]$  are displayed in Fig. 1 showing a clear Bragg structure. The observed spacing corresponds to periodicity of, respectively, 2.36, 2.82, and 4.11 Å in good agreement with the lattice structure of silver shown in Fig. 2. As for the previously reported results on alkali-halides [5,6], the Bragg structure sits on a diffuse background corresponding

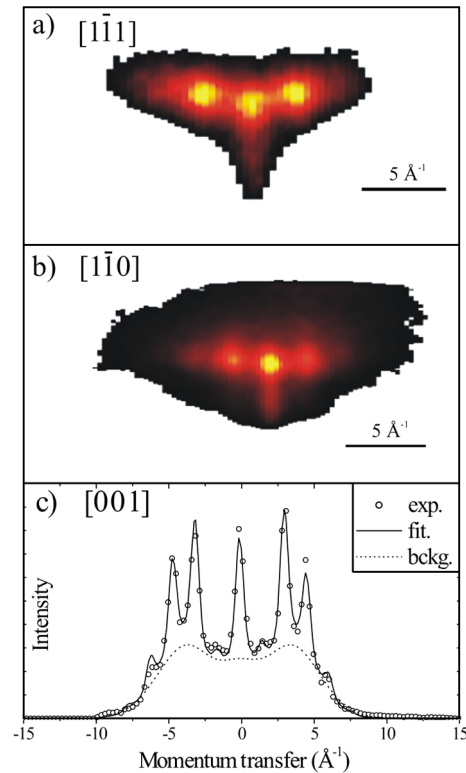


FIG. 1 (color online). Diffraction patterns recorded on a Ag(110) surface for three different directions of the He beam. From top to bottom, the total energy is 1000, 500, and 500 eV while the angle of incidence is  $1^\circ$ ,  $1^\circ$ , and  $0.75^\circ$  so that the normal energy is 360, 180, and 86 meV, respectively. (a) and (b) are 2D raw images, whereas (c) is an intensity plot of a horizontal slice showing the experimental data together with a fit by Gaussians ( $0.5 \text{ \AA}^{-1}$  fwhm) whose relative weight is given by a Bessel function and an estimate of the incoherent background (bckg.). The argument of the Bessel function corresponds to a trough-to-peak corrugation of  $0.31 \text{ \AA}^{-1}$  while the fraction of coherent signal is evaluated here to 36%.

to the incoherent scattering contribution. Surprisingly enough, as shown in Fig. 1(c), the relative contribution of the coherent signal is of the order of 50%, comparable to that previously measured on alkali-halides suggesting that inelastic contributions from electron-hole excitation have a limited effect on the signal coherence. For a given normal energy, the highest order peak corresponds to the classical rainbow angle of the helium-surface potential [17], providing at a glance an estimate of the corrugation. A much more detailed description of the shape of the interaction potential between the helium atom and the surface can be derived from the relative intensities of the peaks. A detailed treatment is beyond the scope of the present paper but a simple approach proven to be qualitatively correct is the Hard Wall model, which considers that the helium atom is reflected by a hard surface. Restricting to the simplest case of a pure sinusoidal corrugation where the only parameter is the trough-to-peak height called hereafter cor-

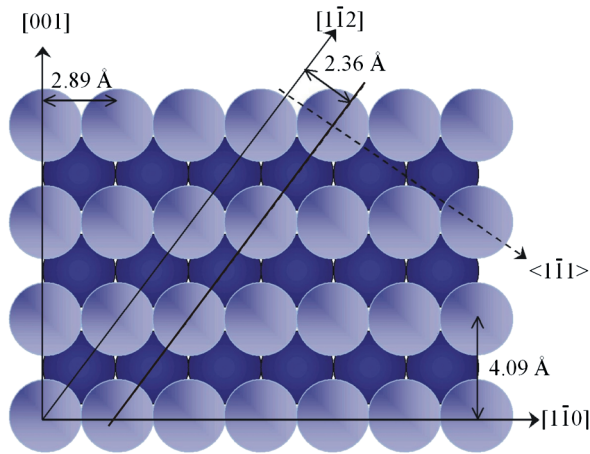


FIG. 2 (color online). Sketch of the Ag(110) surface with its top rows of atoms. For a helium beam aligned along the  $[1\bar{1}0]$ ,  $[001]$ , and  $[1\bar{1}2]$  directions (arrows), the surface is probed in the perpendicular direction, i.e.,  $[001]$ ,  $[1\bar{1}0]$ , and  $\langle 1\bar{1} \rangle$ , respectively. The double-sided arrows indicate the transverse periodicity resulting from averaging along the projectile direction.

rugation, the intensities of the Bragg peaks are simply given by a Bessel function [6,18]. As explained above, the corrugation measured here corresponds to that of the interaction potential averaged along the beam direction and can be quite different from that of slices as measured in TEAS. Yet, along the  $[001]$  axis, comparison to TEAS data should be relevant since the corrugation of the potential varies only slightly along the beam direction, as confirmed by computing the 3D He-Ag interaction potential derived from thermal diffraction [19]. Indeed, at the lowest normal energy of 30 and 86 meV investigated here, the corrugation parameter along the  $[001]$  direction amounts to 0.25 and 0.31 Å, respectively, closely matching that of 0.27 Å obtained at 63 meV from TEAS [20]. It is worth mentioning that diffraction is observed up to 0.5 eV normal energy, almost 10 times higher than in TEAS and without any surface cooling. Obviously, the role of electronic excitation is therefore not as dramatic as could have been anticipated.

By chopping the  $\text{He}^+$  ion beam before neutralization the arrival time of the scattered atoms can be converted in an energy loss spectrum. At 500 eV and  $1^\circ$  incidence, the mean energy loss is close to 1 eV so that electronic excitations are probably low enough to have a negligible contribution on decoherence. This is not the case at 1 and 2 keV where Fig. 3 shows a comparatively broad energy loss structure peaking, respectively, around 3 and 11 eV. Since the recoil energy transferred to the surface atoms can be neglected [21] one can focus on the sole contribution of electronic excitations. A simple model relating inelastic processes to both energy loss and decoherence is that of the binary scattering of an electron on a helium atom (with velocity  $v_p$  in the  $X$  direction). In an isotropic bulk the electron initial wave vector would be inside the Fermi

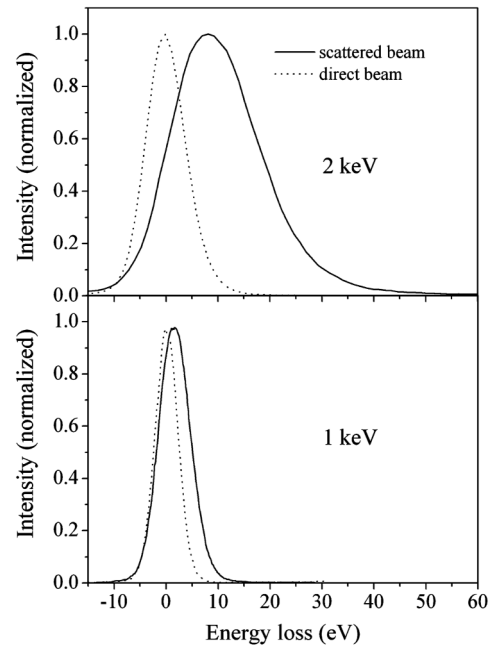


FIG. 3. Energy loss spectra of 1 and 2 keV He scattered off the Ag(110) surface along the  $[1\bar{1}0]$  direction.

sphere while final empty states only exist in the tiny cap delimited by a Fermi sphere shifted by  $2v_p$  [11,22] therefore favoring momentum exchange in the forward direction (i.e.,  $X$ ). Because of the large initial momentum of the projectile in this direction, these collisions have the largest contribution to the energy loss but affect much less the  $k_y$  component whose broadening would wash out the Bragg structure as soon as its magnitude compares with that of a reciprocal lattice vector. Although this model may be sufficient for bulk description, it is not suitable for treating the response of electrons at the classical turning point around 2–3 Å from the surface plane, where the electronic density is as low as  $10^{-3}$ – $10^{-4}$  a.u.. The projectile atom will dominantly encounter electrons spilling out, meaning that their wave function has a comparatively large momentum component normal to the surface ( $k_z$ ), and consequently a lower one in the surface plane ( $k_x$ ,  $k_y$  components). This should limit both the energy loss (change of  $k_x$ ) and the decoherence ( $k_y$  straggling). Although occupied surface states were found to contribute to the energy loss of higher energy protons on Cu(111) [23] our results indicate that, if involved, these states do not induce decoherence. The other explanation of the limited decoherence observed here is more specific to the electronic structure of silver. Both photoelectron spectroscopy and metastable deexcitation spectroscopy [24,25] indicate that the surface density of states exhibits a low density plateau down to 4 eV below the Fermi level. This may act as a pseudo band gap for electron-pair production. Finally a regime governed by multiple but weak momentum trans-

fers could hold in the low electron density region and limit the  $k_y$  broadening. Altogether there are several arguments to explain why the contribution of binary electron scattering to the  $k_y$  straggling is not as efficient as it could be. These mainly outline the need of a consistent treatment of the electron density and momentum distribution at the selvedge of the surface electron density. Reproducing altogether the diffraction signal, the energy loss and decoherence will bring more constraint to theory and most likely contribute to a deeper understanding of the surface electronic properties.

In conclusion, we have demonstrated that against expectations, diffraction of fast atoms can be observed in grazing scattering from a metal surface with a large contrast and a large normal energy range even at room temperature. On Ag(110), diffraction profiles measured below 2 keV show resolution and contrast comparable to those obtained on alkali-halides [5,6], suggesting that electron-hole production have a limited influence on the coherent scattering. The paradox is that the energy loss measurements show significant electronic excitations that could be large enough to wipe out diffraction features.

A better understanding of the exact causes will require a refined modeling of the electron excitation mechanisms where the highly anisotropic surface electronic density together with the momentum density will be described in a self consistent way. Experimentally, the large number of diffraction orders should allow a detailed analysis of the interaction potential over 1 order of magnitude of normal energies. The combined treatment of the scattering, energy loss and decoherence parameters appear challenging and propitious to refined developments. New experiments on metal surfaces with different electronic densities of states and different momentum distribution at the surface may also contribute to understand the limiting factor for diffraction. Finally these new results, besides extending the application potential of grazing incidence diffraction, open new possibilities for fundamental studies of decoherence phenomena in quantum scattering.

A. G. Borisov is gratefully acknowledged for fruitful and numerous discussions along this work as well as V. Esaulov for providing us with the Ag(110) single crystal.

---

[1] C. Davisson and L. H. Germer, Phys. Rev. **30**, 705 (1927).

[2] I. Estermann and O. Stern, Z. Phys. **61**, 95 (1930).

- [3] F. Hofmann, J. R. Manson, and J. P. Toennies, J. Chem. Phys. **101**, 10 155 (1994).
- [4] G. Vidali and C. Hutchings, Phys. Rev. B **37**, 10 374 (1988).
- [5] A. Schuller, S. Wethekam, and H. Winter, Phys. Rev. Lett. **98**, 016103 (2007).
- [6] P. Rousseau, H. Khemliche, A. G. Borisov, and P. Roncin, Phys. Rev. Lett. **98**, 016104 (2007).
- [7] A. Schuller and H. Winter, Phys. Rev. Lett. **100**, 097602 (2008).
- [8] P. Rousseau, Ph.D. thesis, Universite Paris-Sud, 2006.
- [9] J. Manson, H. Khemliche, and P. Roncin, Phys. Rev. B. **78**, 155408 (2008).
- [10] P. M. Echenique, R. M. Nieminen, and R. H. Ritchie, Solid State Commun. **37**, 779 (1981).
- [11] H. Winter and H. P. Winter, Europhys. Lett. **62**, 739 (2003).
- [12] S. M. Ritzau, R. A. Baragiola, and R. C. Monreal, Phys. Rev. B **59**, 15506 (1999).
- [13] C. Auth, A. Mertens, H. Winter, and A. G. Borisov, Phys. Rev. Lett. **81**, 4831 (1998).
- [14] P. Roncin, J. Villette, J. P. Atanas, and H. Khemliche, Phys. Rev. Lett. **83**, 864 (1999).
- [15] H. Khemliche, P. Rousseau, V. Etgens, and P. Roncin (to be published).
- [16] S. Lederer, H. Winter, and H. P. Winter, Nucl. Instrum. Methods Phys. Res., Sect. B **258**, 87 (2007).
- [17] A. Schuller, G. Adamov, S. Wethekam, K. Maass, A. Mertens, and H. Winter, Phys. Rev. A **69**, 050901(R) (2004).
- [18] R. I. Masel, R. P. Merrill, and W. H. Miller, Phys. Rev. B **12**, 5545 (1975).
- [19] M. G. Dondi, S. Terreni, F. Tommasini, and U. Linke, Phys. Rev. B **37**, 8034 (1988).
- [20] A. Luntz, L. Mattera, M. Rocca, S. Terreni, F. Tommasini, and U. Valbusa, Surf. Sci. **126**, 695 (1983).
- [21] H. Winter, A. Mertens, R. Pfandzelter, and V. Staemmler, Phys. Rev. A **66**, 022902 (2002).
- [22] A. G. Borisov, D. Teillet-Billy, and J. P. Gauyacq, Phys. Rev. Lett. **68**, 2842 (1992).
- [23] M. Alducin, V. M. Silkin, J. I. Juaristi, and E. V. Chulkov, Nucl. Instrum. Methods Phys. Res., Sect. B **193**, 585 (2002).
- [24] G. Panaccione, G. Cautero, M. Cautero, A. Fondacaro, M. Grioni, P. Lacovig, G. Monaco, F. Offi, G. Paolicelli, M. Sacchi, N. Stojic, G. Stefani, R. Tommasini, and P. Torelli, J. Phys. Condens. Matter **17**, 2671 (2005).
- [25] L. Pasquali, M. C. Sapet, E. M. Staicu-Casagrande, P. Cortona, V. A. Esaulov, S. Nannarone, M. Canepa, S. Terreni, and L. Mattera, Nucl. Instrum. Methods Phys. Res., Sect. B **212**, 274 (2003).